Supporting Materials

Kinetics of High Density Functional Polymer Nanocomposite formation by Tuning Enthalpic and Entropic Barriers

Aparna Swain,[†] Nimmi Das A,[†] Sivasurender Chandran,[§] and J. K. Basu[*,†]

†*Department of Physics, Indian Institute of Science Bangalore, 560012, India*

‡*Department Physik, Universität Siegen, Walter-Flex-Strasse 3, 57072 Siegen, Germany*

¶*Deutsches Elektronen-Synchrotron, Notkestrasse 85, 22607 Hamburg, Germany*

§*Department of Physics, Indian Institute of Technology Kanpur, Uttar Pradesh 208016, India*

E-mail: basu@iisc.ac.in

Abstract

This supporting document includes information on sample preparation, characterization of PGNP membranes and substrates, information on measurement techniques such as atomic force microscopy, which was used to investigate the evolution of surface morphology of bilayer samples. The details of molecular dynamics simulation performed on bilayer systems with snapshots of the nanoparticle penetration, are also provided here.

Sample preparation

All experiments are carried out on a ultra-thin layer of polystyrene grafted gold nanoparticles (PGNPs) transferred on polymer substrates. PGNPs were synthesized through a modified grafting-to-method as given in the literature. As synthesized particles are dried under vacuum and characterized through various techniques to remove any traces of solvent, and characterized through a palette of techniques to measure their overall size, core size, density of grafted polymers, and the glass transition temperature of the respective membranes. The UV visible spectroscopy of PGNPs are shown in Fig. S1(a). PGNPs are characterized using Transmission Electron Microscopy (TEM), Thermo Gravimetric Analysis (TGA) and Small Angle X-ray Scattering (SAXS). NP core size is deduced from TEM. TEM images of PGNPs with graft molecular weight M_{w} = (3 kD), and (53kD) is given in figure S1(b)-(c). The distribution of the core sizes of respective PGNPs were shown aside of the images.

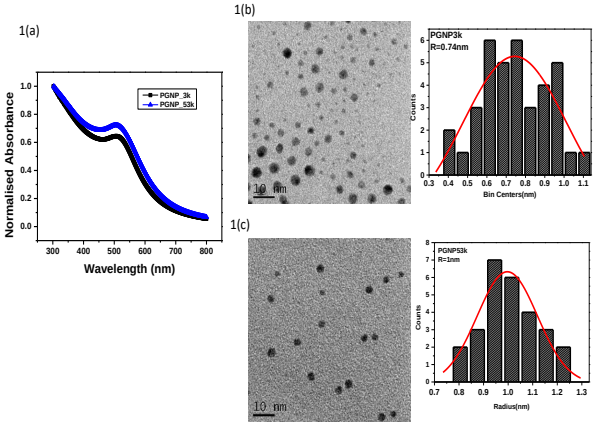

Figure 1: a) Absorption spectra of PGNP-S and PGNP-L collected using UV-visible spectroscopy. TEM images of b) PGNP-S and c) PGNP-L. The size distribution of respective PGNPs were shown aside of the images.

Characterization of PGNPs

TGA (Figure S2(a)) was performed to deduce the mean weight fraction of Au core and PS corona in the PGNPs. Grafting density of PGNPs were estimated using Au fraction from TGA and core size from TEM. We SAXS (Bruker, Nanostar Germany) to measure the overall PGNP size combining both the core and the polystyrene shell. SAXS profiles (intensity vs wave vector) of powder samples of different PGNPs, shown in (Figure S2(b)) captures the structure factor peak characterizing the mean separation between two neighboring PGNPs, which is equivalent to the diameter of the PGNP in powder form.

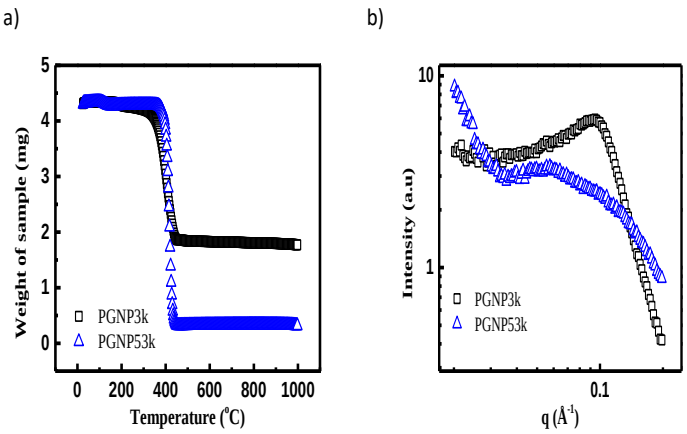

Figure 2: a) TGA and b) SAXS data of all PGNPs. All symbols are defined in respective panels.

Preparation of supported PGNP membranes

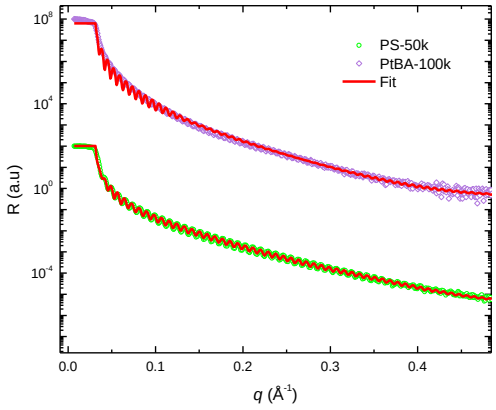

Figure 3: X-ray reflectivity and respective fits (red curve) used for estimation of polymer substrate thickness.

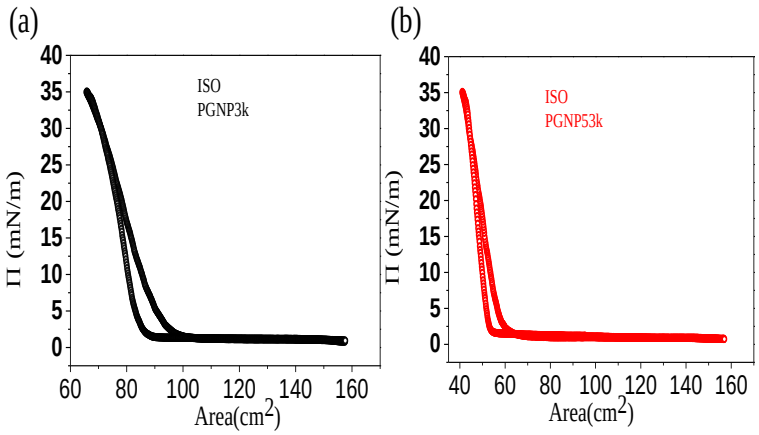

Figure 4: Iso curve of monolayer of (a)PGNP3k and (b)PGNP53k. surface pressure vs area.

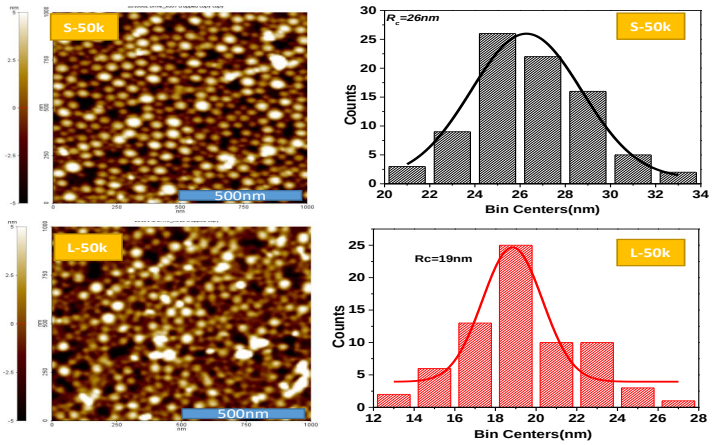

Figure 5: AFM images of as transferred S-50k and L-50k with grain size histograms. The grain radius is estimated from the histogram.

Table 1: Specifications of PGNPs and constituting monolayer

PGNP	M_w of shell [kDa]	r_{Au} [nm]	h_s [nm]	r_c [nm]
S	3	1.7	1.6	26
L	53	0.9	4.4	19

Here r_{Au}: radius of Au core with error of 0.4 nm, h_s: shell thickness with error of 0.6 nm, r_c: radius of PGNP cluster with error of 3. Naming of monolayer: S - small molecular weight, 3 kDa; L - large molecular weight, 53 kDa. Sample naming is adapted from our earlier work.[1]

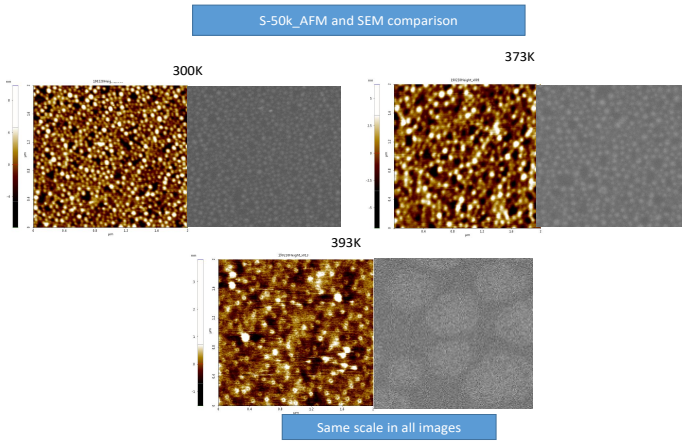

Figure 6: SEM and AFM images of S-50k at a) $T = 300$ K, b) $T = 373$ K and c) $T = 393$ K.

Controlled experiment of Temperature and time dependent AFM imaging to see the penetration of nanoparticles from the structural changes on the surface

We have done the temperature dependent AFM in the presence of N_2 gas flow. The temperature is increased at the rate of 1 degree/min. Temperature induced structural changes for L-50k and L-PtBA samples are given in Fig. S7 and S8. As temperature of the system increases towards substrate T_g, the grains are penetrating into the bottom membrane and the surface is becoming smooth like a pure polymer surface. So, we have done the controlled experiment near the transition temperature of the membrane to compare the entropic and enthalpic effect on penentration of PGNPs. We have also quantify the normalised height vs temperature for all the samples and fitted with sigmodal function to get the transition temperature.

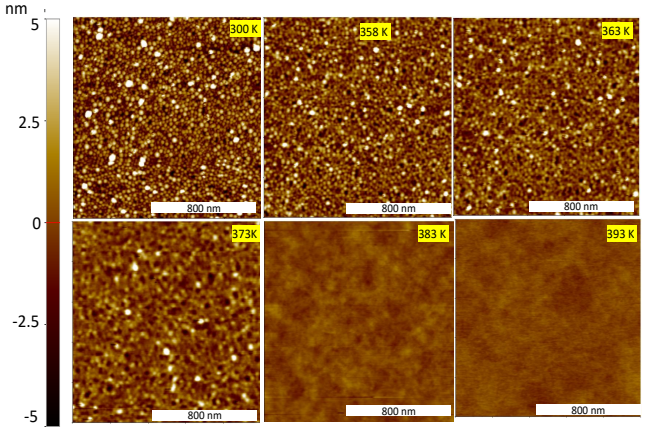

Figure 7: The AFM images of L-50k with temperatures.

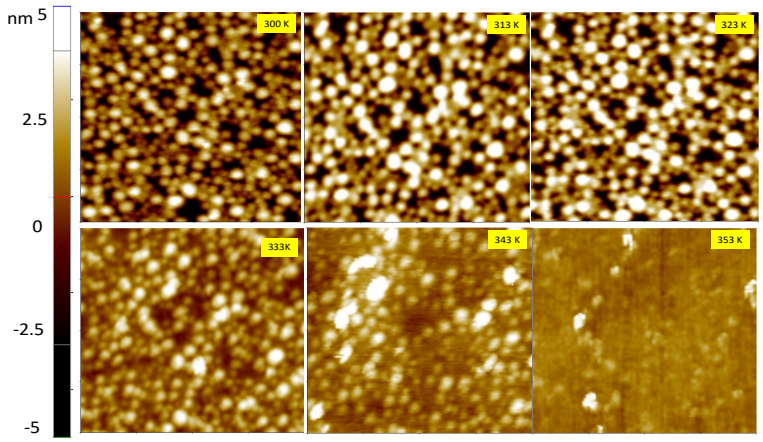

Figure 8: The AFM images of L-PtBA with temperatures.

3D View of AFM images and comparison of surface height with temperature and time

To understand the effect of entropic and enthalpic barrier on penetration of PGNPs, We have collected AFM images at regular time intervals near the transition temperature (Fig. S9-S12). On comparing S-50k and L-50k at $T = 363$ K (Fig. S9 and S10), we can see that PGNP penetration is faster in L-50k as compared to S-50k. On the other hand, for PtBA based samples we observe that the grains in L-PtBA is penetrating slower than that of S-PtBA (Fig. S11 and S12). In figure S12, the comparison of surface height histograms are given.

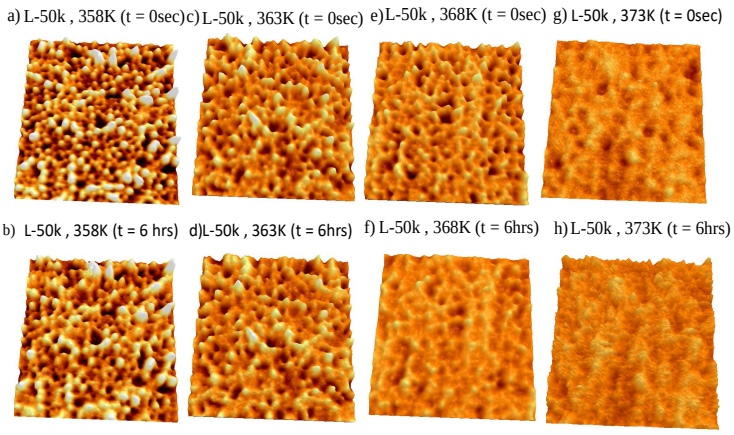

Figure 9: AFM 3D view of L-50k. The temperature and timescales are mentioned in the figure.

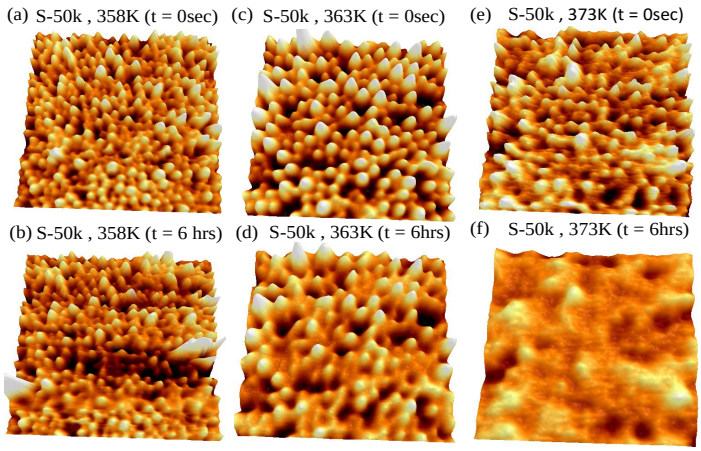

Figure 10: AFM 3D view of S-50k. The temperature and timescales are mentioned in the figure.

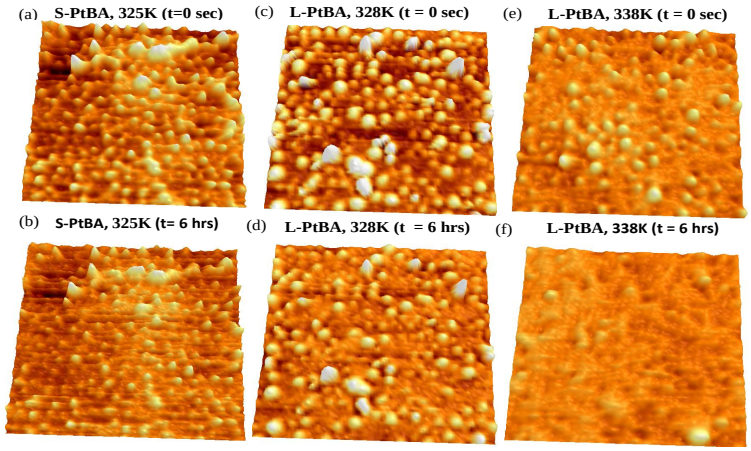

Figure 11: AFM 3D view of S-PtBA a) T = 324 K (t = 0 hrs), b) T = 324 K (t = 6 hrs), c) L-PtBA, T = 328K (t=0 hrs), d)T = 328K (t = 6 hrs), e) L-PtBA, T = 338K (t=0 hrs) f) T = 338K (t = 6 hrs).

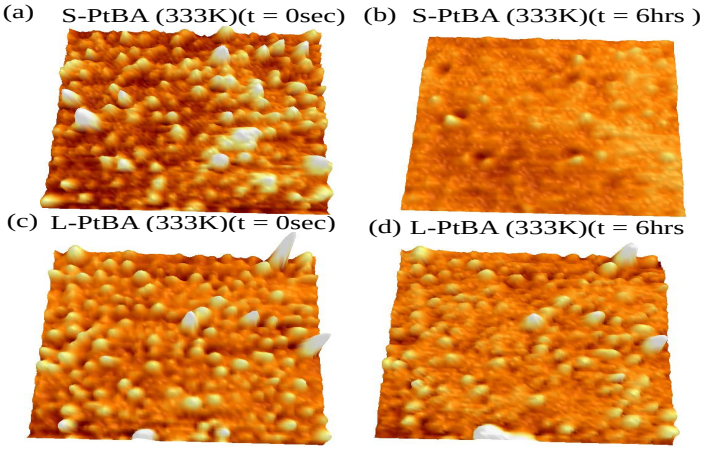

Figure 12: AFM 3D view for S-PtBA a) T = 333 K (t = 0 hrs), b) after (t = 6 hrs), c) for L-PtBA T = 333 K (t=0 hrs), d) after (t = 6 hrs).

Comparison of height histogram at similar timescales

To compare the penetration of nanoparticles into the bottom bulk polymer, we have shown the height histogram with temperature for both the systems.

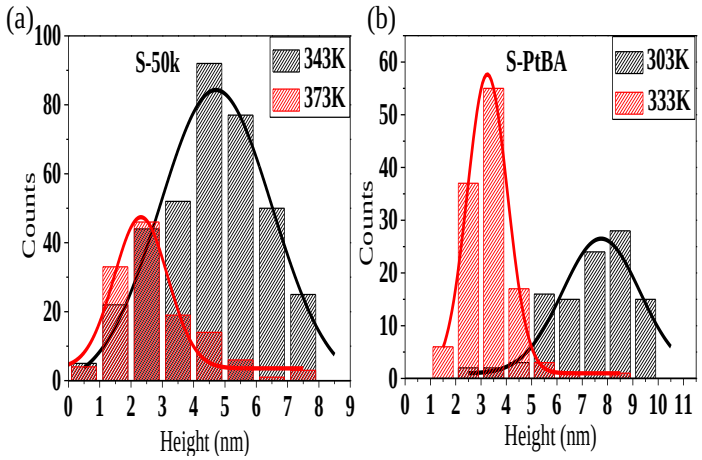

Figure 13: The height histogram of a) S-50k at temperature 343K and 373K and b) S-PtBA at temperature 303K and 333K. The temperature mentioned in the figure.

The height histogram for all the samples at time evolution. We can clearly see the height as well as width are changing with time.

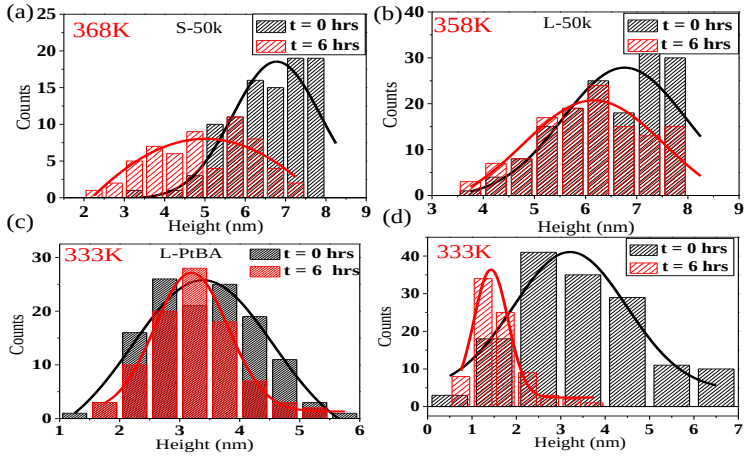

Figure 14: The height histogram of a) S-50k at temperature 368K b) L-50k at 358K c) L-PtBA at 333K and d) S-PtBA at temperature 333K. The temperature and timescales are mentioned in the figure.

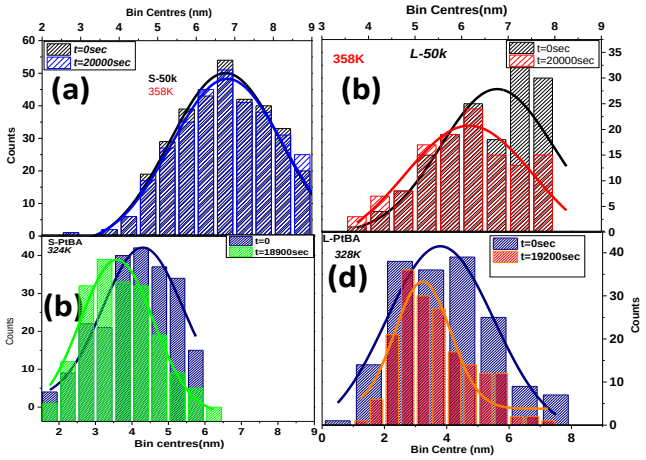

Figure 15: The height histogram of a) S-50k, b) L-50k, c) S-PtBA, and d) L-PtBA. The temperature and timescales are mentioned in the figure.

Relaxation time of pristine polymers

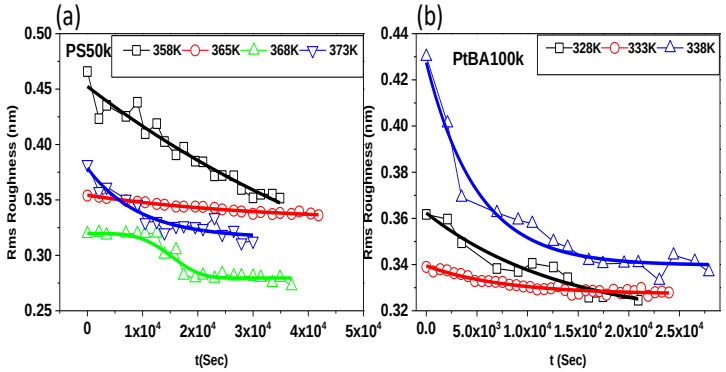

Figure 16: The rms roughness obtained from AFM images as a function of time for pristine polymer a) PS50k and b) PtBA100k. The temperatures are mentioned in the figure. The solid line is the fit using exponential decay function.

The rms roughness obtained from AFM images as a function of time for pristine polymers are shown in Fig. S13. We find that roughness decays exponentially with temperature.

The surface height as a function of time

Here we have shown the temporal evolution of surface normalised height $(h(t)/h(t0))$ of bilayer films at different temperatures. On comparing PS based samples, it is very clear that

the penetration of PGNPs is faster in L-50k than that of S-50k. On contrary, the behavior is opposite in PtBA based samples, the penetration is slower in L-PtBA as compared to S-PtBA.

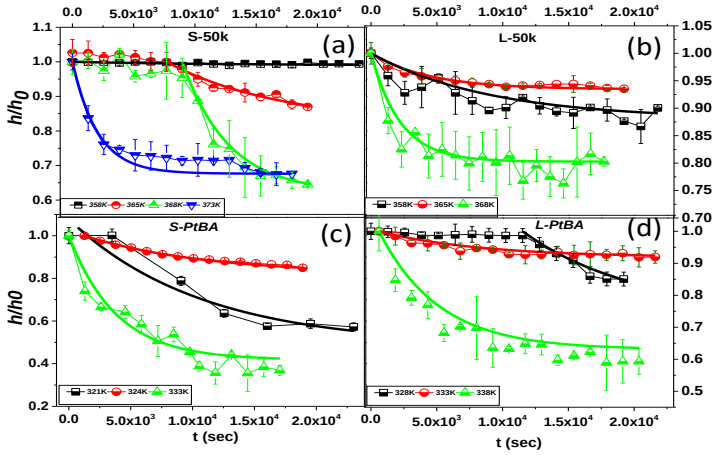

Figure 17: The surface height as a function of time for a) S-50k, b) L-50k, c) S-PtBA, and d) L-PtBA.

Comparison of percentage of penetration

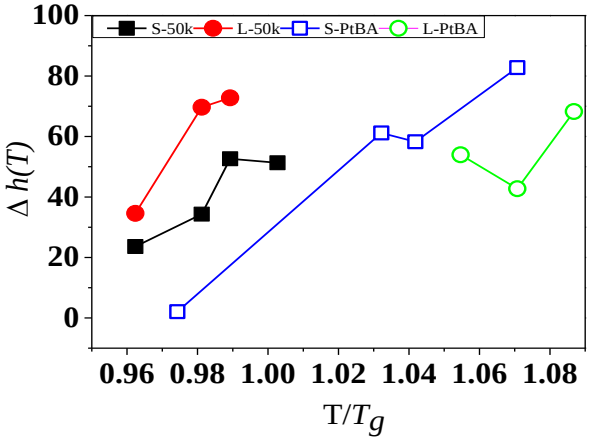

Figure 18: The percentage of penetration, Δh as a function of T/T_{g} for bith PS based and PtBA based samples.

To quantify the penetration of PGNPs into the bulk, we estimate the percentage of penetration, Δh, using the following relation,

$$\Delta h(T) = \left[\frac{h(T = 303K, t = 0) - h(T, t = 6hrs)}{h(T = 303K, t = 0)}\right] * 100, \quad (1)$$

An overall increase in the percentage of penetration with temperature is observed for all samples, as expected (Fig. S15). Within PS based samples PGNP penetration is faster in L-50k and the trend is opposite in PtBA based samples.

MD simulation

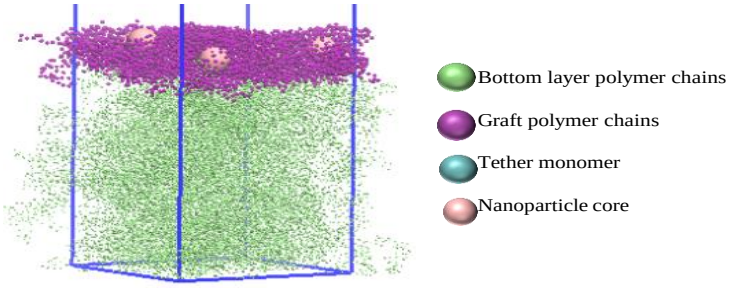

Figure 19: Snapshot of simulation system: monolayer of polymer grafted nanoparticles resting on top of a thick polymer layer. This snapshot is created using Visual Molecular Dynamics (VMD) software. Here, graft chain has 53 monomers and the bottom layer polymer chain has 50 monomers. Different monomer size is chosen for clarity and hence size of the monomers shown in the picture has no correlation with actual monomer size.

In order to confirm the experimental observations, we have performed coarse grained molecular dynamics (MD) simulations using LAMMPS simulator.[2] The bilayer consists of a mono layer of PGNPs on top of a bulk free linear chains inside a rectangular box with periodic boundary conditions along X and Y-direction and a fixed boundary condition is applied along Z-direction. We use canonical NVT ensemble in which the amount of Particle , Volume of simulation box and temperature is kept constant. To maintain a constant temperature vari-

ety of thermostat exists,the commonly use one is the Nose-Hover thermostat. To make the linear chains we have used the bead-spring model with hybrid potential of finite extensible nonlinear elastic (FENE) potential and harmonic potential with standard values of the parameters.[3] All the species of the system interacted through shifted Lennard-Jones potential with the following equation,[4]

$$E = 4\epsilon\ [(\frac{\sigma}{r})^{12} - (\frac{\sigma}{r})^{6}] - E_{\mathrm{rc}}, \tag{2}$$

where $rc = ((D1 + D2)/2)\sigma$ ($D1$ and $D2$ are the diameter of the interacting species and σ is the length unit), E_{rc} is the energy cut-off at $r = rc$ and ϵ is the reduced energy unit. The non-bonded graft-graft monomer interactions were modeled using Lennard-Jones potential with $\epsilon_{gg} = 1.0k_BT$. To model PGNP/PS$^{\mathrm{sim}}$ system, non-bonded matrix-matrix and graft-matrix interactions were set as Lennard-Jones potential with ϵ_{mm} and ϵ_{mg} at $1.0k_BT$ and $1.03k_BT$, respectively. Whereas to model PGNP/PtBA$^{\mathrm{sim}}$ system, non-bonded matrix-matrix and graft-matrix interactions were set as Lennard-Jones potential with $\epsilon_{mm} = 0.83k_{\mathrm{B}}T$ and $\epsilon_{mg} = 0.7k_{\mathrm{B}}T$ respectively. The temperature of the system is kept at $T/T_{\mathrm{g}} \approx 1.09$, where T_{g} of PS and PtBA is 0.44 and 0.37 receptively in reduced units.[5] The initial snapshot of the bilayer system before production runs is shown in Figure S16.

The snapshot of time evolution of PGNP-PS$^{\mathrm{sim}}$ and PGNP-PtBA$^{\mathrm{sim}}$ bilayer systems are shown in Figure S17 respectively.

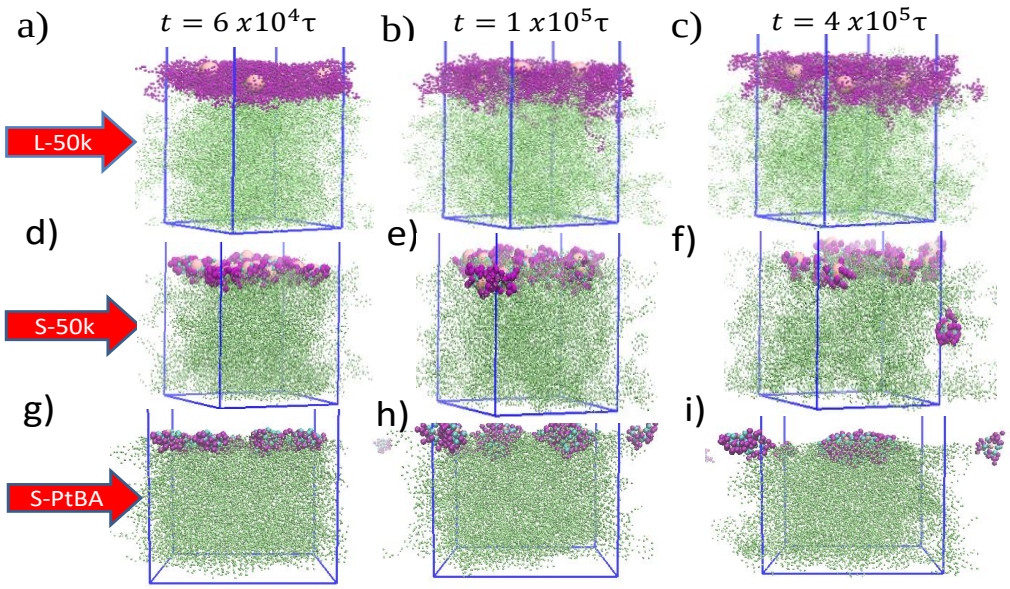

Figure 20: The VMD snapshot of bilayer samples at different time scales. (a-c) L-50k at $T/T_g \approx 1.36$, (d-f) S-50k at $T/T_g \approx 1.36$ and (g-i) S-PtBA system at $T/T_g \approx 1.09$. Time is mentioned in the figures.

From MD simulation we have extracted the nanoparticle number density along the thickness of bilayer (Fig. S19 and S20). The peak in the profile indicates the location of top PGNP layer and the increase in the peak width indicates the penetration of nanoparticles into the bottom polymer layer. The width of nanoparticle peak in L-50k sample increases with time very quickly as compared to S-50k indicating fast nanopaticle penetration in L-50k as compared to S-50k. For quantify the penetration of nanoparticles into the bulk, we are defining the surface region from the profile as the position of the peak and following the evolution of the peak only in that region. In Fig. S21, we have shown the surface density area reduction with time for S-50k and L-50k.

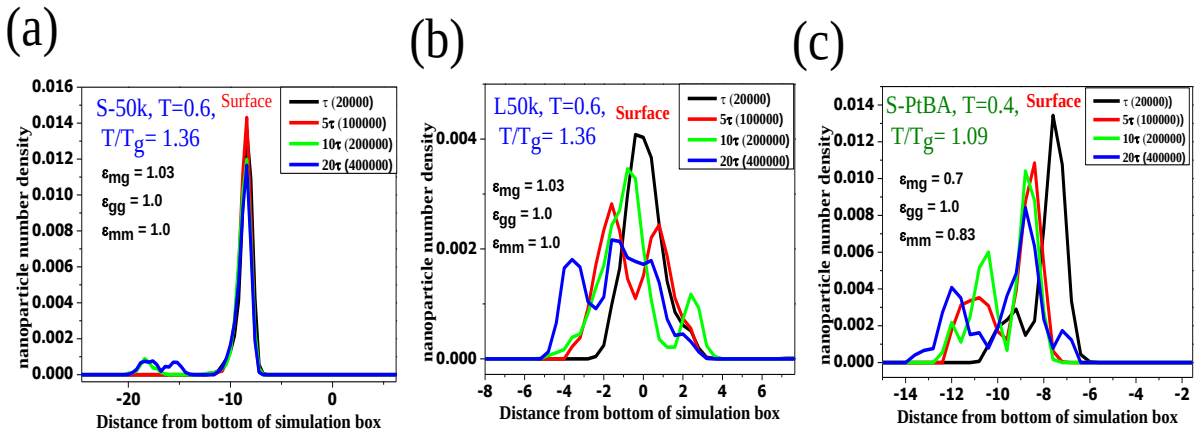

Figure 21: The nanoparticle number density profile of a) S-50k, (b) L-50k, and (c) S-PtBA along the bilayer thickness. All the parameters are mentioned in the figures.

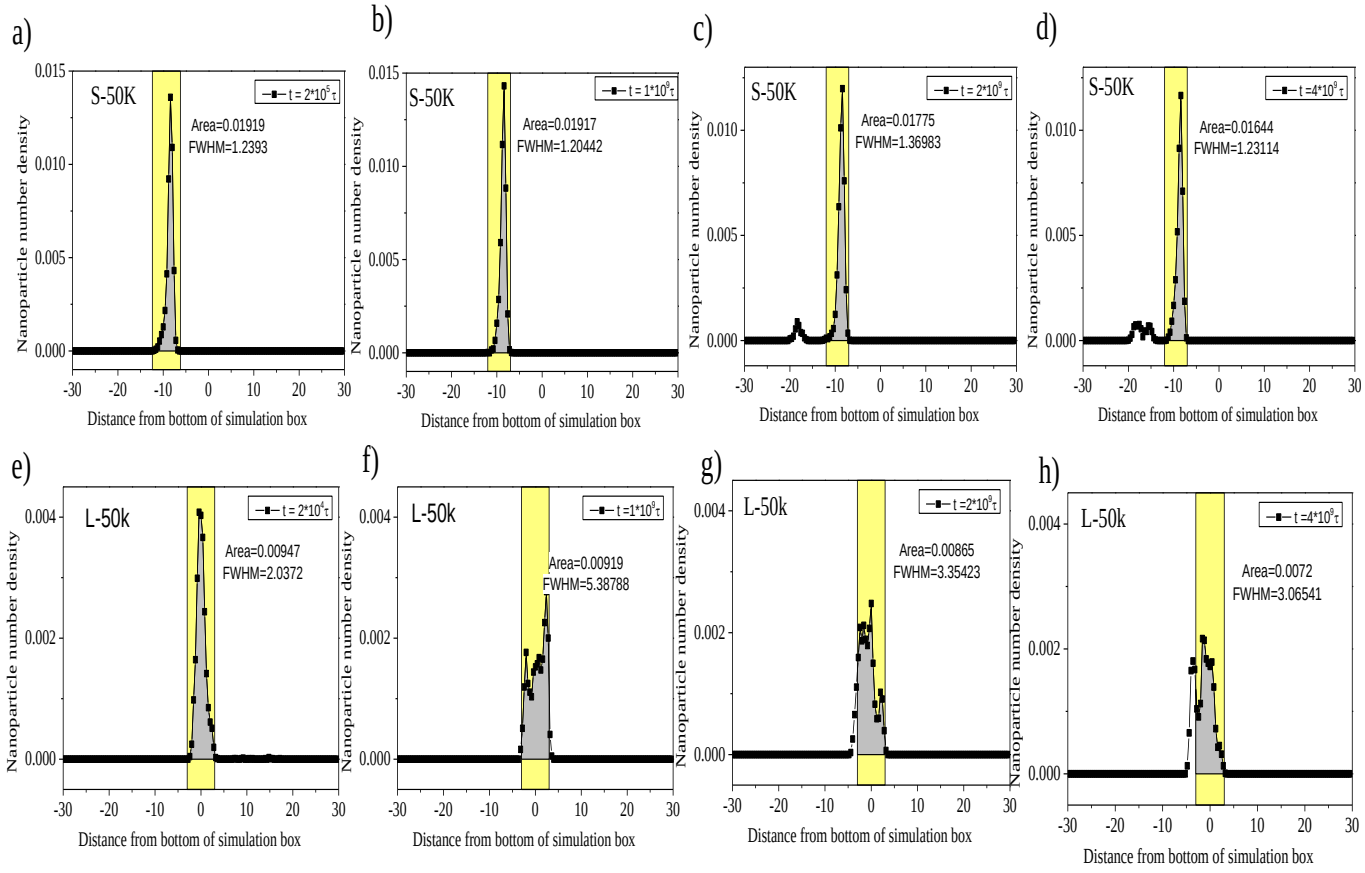

Figure 22: The nanoparticle number density profile of a) S-50k and b) L-50k at different time scales.

References

(1) Das, N.; Begam, N.; Chandran, S.; Swain, A.; Sprung, M.; Basu, J. K. Thermal stability and dynamics of soft nanoparticle membranes: role of entropy, enthalpy and membrane compressibility. *Soft Matter* **2020**, *16*, 1117–1124.

(2) Ibrahim, M.; Begam, N.; Padmanabhan, V.; Basu, J. K. Correlation between grafted nanoparticle–matrix polymer interface wettability and slip in polymer nanocomposites. *Soft matter* **2018**, *14*, 6076–6082.

(3) Kremer, K.; Grest, G. S. Dynamics of entangled linear polymer melts: A molecular-dynamics simulation. *J. Chem. Phys.* **1990**, *92*, 5057–5086.

(4) Padmanabhan, V.; Frischknecht, A. L.; Mackay, M. E. Effect of chain stiffness on nanoparticle segregation in polymer/nanoparticle blends near a substrate. *Macromol. Theory Simul.* **2012**, *21*, 98–105.

(5) Das, N.; Swain, A.; Begam, N.; Bhattacharyya, A.; Basu, J. K. Temperature-Driven Grafted Nanoparticle Penetration into Polymer Melt: Role of Enthalpic and Entropic Interactions. *Macromolecules* **2020**, *53*, 8674–8682.